# BER Analysis of ASK and BPSK Modulation over the *Dyadic Backscatter* Channel in UHF RFID

**Aisyah Novfitri[1*], Kamelia Quzwain[2], Septriandi Wirayoga[3], Seshariana Rahma Melati[4]**
[1,2,4]Telecommunication Engineering Study Program, Telkom University, Jakarta, Indonesia
[3]Department of Electrical Engineering, State Polytechnic of Malang, Malang, Indonesia
E-mail: [1*]aisyahnovf@telkomuniversity.ac.id, [2]kquzwain@telkomuniversity.ac.id, [3]yoga.septriandi@polinema.ac.id,
[4]sesharianarahmam@telkomuniversity.ac.id

***Abstract*— Passive UHF RFID tags communicate by backscatter, so the signal crosses the channel twice, yet most bit error rate analyses still treat the channel as a single path. This study quantifies the cost of that simplification for MLFF toll portals. The BER of amplitude shift keying (ASK) and binary phase shift keying (BPSK) over a dyadic backscatter channel is evaluated by Monte Carlo simulation. Single-path modeling underestimates the required power by 8.2 dB for BPSK and 8.4 dB for ASK without a line-of-sight component, a read-range loss of about 38 percent on the two-way path scale. The fading margin relative to the AWGN channel is independent of the modulation (maximum deviation 0.3 dB), so modulation and channel can be budgeted separately. Margin sensitivity to the Rician K-factor peaks between K = 6 and 8 dB and falls sharply above 12 dB, so a portal should keep K at 12 dB or more for a margin below 3 dB. Full inter-link correlation in a monostatic reader halves the diversity order to 0.5, with a penalty of about 19 dB at a BER of 0.001 that grows as the target BER is tightened, making separate transmit and receive antennas a design requirement.**

***Keywords—UHF RFID, dyadic backscatter channel, bit error rate, Rician factor, link correlation***

## I. INTRODUCTION

The roll-out of the barrier-free *Multi-Lane Free Flow* (MLFF) toll system in Indonesia calls for vehicle identification that stays reliable at speed, with no stopping; the average vehicle speed on the national toll network is about 65.3 km/h [1]. A missed read has two costs: the operator loses revenue on a vehicle that passes unrecorded, and traffic backs up whenever the system hesitates before opening a gate. *Radio Frequency Identification* (RFID) in the *Ultra High Frequency* (UHF) band, from 860 to 960 MHz, is the leading candidate because it reads at distances of several meters using low-cost passive tags [2], [3]. Unlike *Low Frequency* (LF) and *High Frequency* (HF) RFID, which rely on inductive coupling at short range, UHF RFID is more prone to read failures than a conventional one-way radio link, especially when vehicles pass at high speed, when neighboring vehicles shadow or reflect the signal, and in bad weather. This remains one of the main technical obstacles to fully reliable MLFF operation. Beyond antenna and chip reliability, the two-way nature of passive RFID communication makes it inherently more sensitive to disturbance than its LF and HF counterparts. UHF RFID operates in the far field through modulated *backscatter*: a passive tag has no transmitter of its own, but modulates its antenna impedance to reflect the carrier sent by the reader [2], [4]. A fundamental consequence is that the information signal crosses the propagation channel twice, on the forward link from reader to tag and on the return link from tag to reader, so the fading it experiences is compounded (a *double-fading channel*).

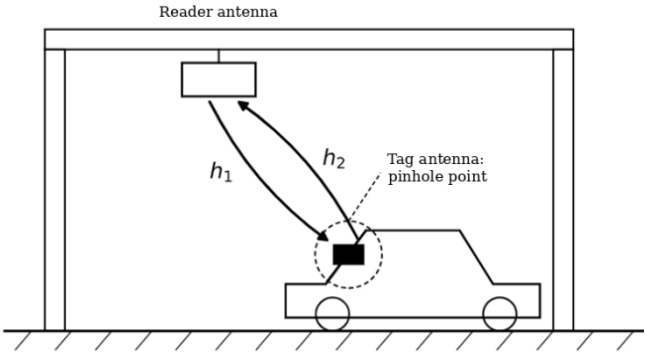



Fig. 1. The *Dyadic Backscatter* channel at an MLFF toll portal

The *dyadic backscatter channel*, the double-fading structure illustrated in Fig. 1, exhibits deeper small-scale fading than a conventional one-way channel [2], [5]. All multipath energy on the forward link must pass through a single narrow point, the tag antenna, before spreading out again on the return link; for this reason it is also known as a *pinhole* channel, and its effective channel coefficient is the product of two random variables, giving a *cascaded fading* distribution [6]. Modeling the channel coefficient as the product of two independent fading terms has become the standard framework for backscatter analysis, including work that couples it with coding, modulation, and energy harvesting at the tag [7]. Although these characteristics have long been established, most *Bit Error Rate* (BER) analyses of UHF RFID systems still model the channel as a single, conventional path. Research over the past decade has broadened backscatter studies to ambient backscatter communication and battery-free *Internet of Things* (IoT) devices [8], [9], [10], but the emphasis there is on system architecture, detection schemes, and energy harvesting rather than on what the channel simplification does to the link budget of a practical UHF RFID deployment. In theory, the *Rayleigh* distribution represents the absence of a line-of-sight path, whereas the *Rician* distribution with factor K represents a dominant line-of-sight component; both serve as the basis for modeling the forward and return links in this study [11], [12].

UHF RFID research for transportation has been most active on the hardware and system-integration side. Reader antenna design for the 923–925 MHz band allocated in Indonesia has been studied through a comparison of elliptical patch configurations and their feeding techniques [13]. At the operational level, the effect of reader transmit power and antenna tilt on the read distance to vehicle tags at an RFID-based toll gate has been measured in the field, with the best configuration of 20 dBm and a 5-degree tilt giving a read range of 6.5 m [14]. Both studies, however, focus on antenna design and system integration rather than on the propagation

channel that underlies the *backscatter* mechanism itself. UHF RFID transmission parameters in an MLFF setting, including the *Received Signal Strength Indicator* (RSSI), *Packet Error Rate* (PER), read rate, and the relationship between Signal-to-Noise Ratio (SNR) and BER, have also been evaluated by combining MATLAB simulation with field measurement [15]. That SNR–BER analysis, however, still assumes a one-way channel with additive noise and ignores the *dyadic backscatter* property, so its recommended SNR threshold of 10 dB is likely to be optimistic relative to the actual power requirement. On the analytical side, closed-form performance of monostatic and bistatic passive UHF RFID over cascaded fading channels has been derived, along with the maximum read range in multipath and interference-limited environments [16], but the metric there is tag detection probability rather than a comparison of the power required by different modulation schemes at a given target BER. Elsewhere, the effect of envelope correlation in a *monostatic reader* with a single-antenna tag has been measured [5], yet the power penalty has not been quantified for the parameters that matter at a high-speed toll gate, such as vehicle speed, effective read range, and angle of arrival, in either the international or the national literature. These gaps motivate the present work, which sits between system-level UHF RFID studies for tolling and the still-limited characterization of the *backscatter* channel: it quantifies the power penalty of Amplitude Shift Keying (ASK) and Binary Phase Shift Keying (BPSK) modulation over the *double-fading backscatter* channel for the operating scenario of MLFF toll gates in Indonesia.

Against this background, the study addresses three gaps: the power penalty incurred by collapsing the *dyadic* channel into a one-way channel, the loss due to inter-*link* correlation for toll-gate reader configurations, and the minimum *Rician* factor that portal geometry should be designed to provide. These are quantified through Monte Carlo simulation, with four contributions. First, the power penalty of *dyadic* modeling relative to one-way modeling is measured for matched link distributions. Second, the dependence of the fading margin on the modulation type is tested. Third, the sensitivity of the fading margin to the *Rician* factor is mapped and a design threshold for toll portals is established. Fourth, the effect of link envelope correlation is analyzed not merely as a curve shift but as a change in *diversity* order.

## II. Materials and Methods

The work proceeds through mathematical channel modeling, Monte Carlo simulation, and validation of the results against theoretical expectations. All simulations were run in MATLAB in three stages: formulating the channel model, generating Monte Carlo realizations, and checking the results against theoretical values. Monte Carlo simulation is used because the BER distribution over a cascaded channel is difficult to obtain in closed form; the method estimates the BER by generating a large number of random realizations of bits, channel, and noise, then taking the ratio of erroneous bits to the total transmitted.

### A. System Model

The system under study is the uplink of a passive UHF RFID link, i.e., data transmission from tag to reader over the *backscatter* channel using ASK and BPSK modulation. Information bits are drawn at random with equal probability and mapped to symbols according to the modulation order. The signal received at the reader is given by (1) [17].

$$r = h\,s + n \tag{1}$$

where $r$ is the received signal, $h$ the effective channel coefficient, $s$ the transmitted symbol, and $n$ the additive white Gaussian noise or AWGN, with the signal energy normalized. The UHF RFID bit rate is 40 kbps in a 200 kHz channel *bandwidth* [18]. The effective *backscatter* channel coefficient $h$ is given by (2) [2].

$$h = h_1 . h_2 \tag{2}$$

where $h_1$ is the forward-link coefficient from reader to tag and $h_2$ the return-link coefficient from tag to reader. Without a line-of-sight path, both coefficients are modeled as complex Gaussian random variables with *Rayleigh*-distributed envelopes, and their product follows a *double Rayleigh* distribution [6]. With a line-of-sight path, both are modeled as *Rician* variables with factor $K$ as given in (3) [12].

$$h_i = \sqrt{\frac{K}{K+1}} + g_i\sqrt{\frac{1}{K+1}} \tag{3}$$

$g_i$ is a zero-*mean* complex *Gaussian* variable and $i$ takes the values 1 and 2 for the two links. Using the same factor $K$ on both links reflects the symmetric geometry of a toll portal, where the reader antenna views the tag on the windshield and both links pass through the same region. For the performance analysis, three channel conditions are simulated: an AWGN channel without fading as the reference, followed by *Rayleigh* and *Rician* channels. Once all Monte Carlo runs are complete, performance is evaluated in terms of BER against the SNR per bit, expressed as the ratio of energy per bit to noise power spectral density ($E_b/N_0$), with a success threshold of $10^{-3}$.

### B. Link Envelope Correlation Model

Inter-link correlation is generated through a complex correlation coefficient as given in (4) [5].

$$h_2 = \rho h_1 + g\sqrt{1-\rho^2} \tag{4}$$

where $\rho$ is the complex correlation coefficient and $g$ an independent complex Gaussian variable. A value of $\rho$ equal to zero represents a reader with separate transmit and receive antennas, while $\rho$ equal to one represents a monostatic configuration in which the same antenna transmits and receives. The mean channel power for two correlated complex Gaussian variables is given by (5).

$$E[|h_1\,h_2\,|^2] = 1 + \rho^2 \tag{5}$$

The mean power of the *dyadic* channel $E$ increases with correlation. Without normalization, part of the correlation loss would be masked by this apparent power gain, so every channel realization is normalized to unit mean power at each correlation value tested. Note that the RFID literature usually reports envelope correlation, i.e., the correlation between the magnitudes of h1 and h2, rather than complex correlation; the two are related through Clarke's approximation, with the envelope correlation approximately equal to the square of the

complex correlation. Numerical verification showed that a complex correlation setting of 0.775 produced a measured envelope correlation of 0.573 against a target of 0.600.

### C. Simulation Parameters

The system parameters, simulation settings, and the design of the three experiments used throughout are summarized in TABLE I.

TABLE I. SIMULATION PARAMETERS AND EXPERIMENTAL DESIGN

| Parameter | Value |
|---|---|
| **System and detection** | |
| Modulation | ASK and BPSK |
| Detection scheme | Coherent |
| BPSK decision threshold | 0 |
| ASK decision threshold | 0.5\|$h$\| (channel-adaptive) |
| **Simulation settings** | |
| Bits per $E_b/N_0$ point | $10^6$ |
| $E_b/N_0$ range | 0–50 dB |
| BER | $\leq 10^{-3}$ |
| **Experimental design** | |
| Experiment A – channel model | AWGN; single *Rayleigh*; single *Rician* (K = 5 dB); *dyadic Rayleigh*; *dyadic Rician* (K = 5 dB) |
| Experiment B – envelope correlation | 0.0; 0.3; 0.6; 1.0 (*dyadic Rayleigh* channel) |
| Experiment C – *Rician* factor | 0; 4; 6; 8; 10; 12; 15; 20 dB (uncorrelated *dyadic Rician* channel) |

### D. Fading Margin and Sensitivity Definitions

The fading margin is the extra $E_b/N_0$ that a fading channel needs, relative to the AWGN channel, to reach the same target BER with the same modulation [2]. For the dyadic Rician channel it is given by (6).

$$M(K) = \Gamma_{\text{dyadic}}(K) - \Gamma_{\text{AWGN}} \tag{6}$$

where $\Gamma$ is the required $E_b/N_0$ at a BER of $10^{-3}$, read from the Monte Carlo BER curves. The sensitivity $S_i$ in TABLE III is the margin improvement per 1 dB increase in $K$ between consecutive rows, computed from the BPSK margins with (7); the first row has no preceding value.

$$S_i = \frac{M(K_{i-1}) - M(K_i)}{K_i - K_{i-1}} \tag{7}$$

## III. RESULTS AND DISCUSSION

### A. Model Validation

The $E_b/N_0$ difference between ASK and BPSK across the sixteen configurations tested lies between 5.7 and 6.3 dB, with a mean of 6.0 dB. The *dyadic Rayleigh* configuration, which appears in two separate experiments, agrees to within 0.3 dB despite different random realizations.

### B. Dyadic Channel Modeling Penalty

Figs. 2 and 3 show the BER versus $E_b/N_0$ curves for the five channel models under BPSK and ASK. The *dyadic* channel curves lie to the right of the one-way curves and have a shallower slope, the hallmark of *cascaded fading*. The results for the different channel conditions and models are summarized in TABLE II.

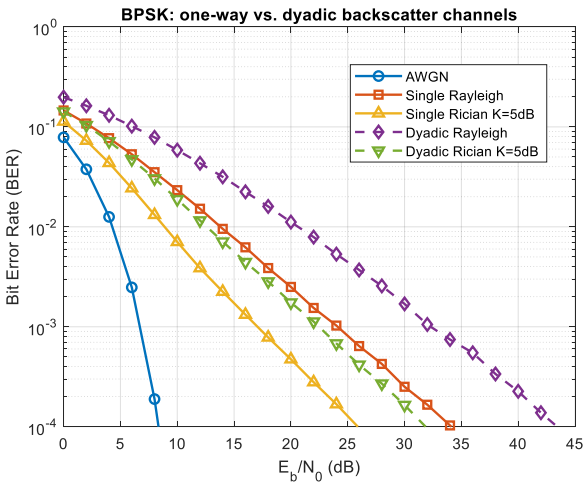



Fig. 2. BER of BPSK over one-way and *dyadic backscatter* channels

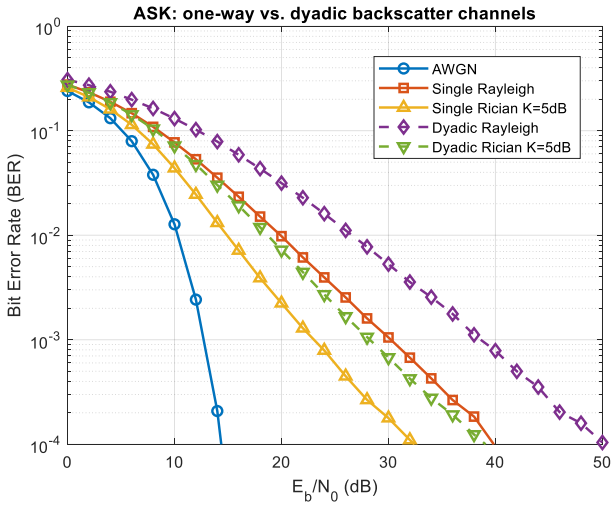



Fig. 3. BER of ASK over one-way and *dyadic backscatter* channels

Based on TABLE II, the $E_b/N_0$ requirements are compared for matched link distributions. Relative to a single *Rayleigh* channel, the *dyadic Rayleigh* channel requires an additional 8.4 dB for ASK and 8.2 dB for BPSK. Relative to a single *Rician* channel with $K$ = 5 dB, the *dyadic Rician* channel with the same K-factor requires an additional 5.3 dB for ASK and 5.4 dB for BPSK. The extra power is needed because in the *dyadic* channel the signal fades on both links at once, leaving it worse off than over a one-way channel.

TABLE II. REQUIRED $E_b/N_0$ AT A BER OF 0.001 FOR THE CHANNEL MODELS

| Channel model | ASK (dB) | BPSK (dB) |
|---|---|---|
| AWGN | 12.7 | 6.7 |
| Single *Rayleigh* | 30.2 | 24.1 |
| Single *Rician*, K = 5 dB | 23.0 | 17.1 |
| *Dyadic Rayleigh* | 38.6 | 32.3 |
| *Dyadic Rician*, K = 5 dB | 28.3 | 22.5 |

An extra 8.2 dB of required power has a large effect on system range. Because the penalty arises at the reader's receiver, after the signal has traveled the forward and return

links, its conversion to distance follows the two-way scale, with received power proportional to $d^{-4}$ in free space. The decibel-to-distance conversion therefore uses 40 dB per decade rather than the 20 dB per decade of a one-way channel. With the transmit power held fixed, an 8.2 dB increase in required power corresponds to a distance factor of 1.60, so the read range shrinks to about 62 percent of its original value, a reduction of about 38 percent; the 8.4 dB ASK penalty gives practically the same figure. This holds when the system range is limited by reader sensitivity on the return link. If the system is instead limited by the tag activation threshold on the forward link, which scales as $d^{-2}$, the same power deficit corresponds to a range reduction of up to about 61 percent. For a passive tag the operating range is set by the weaker of the two links [19], so the 38 percent figure is adopted as the estimate consistent with the two-way channel structure at the heart of this analysis. The true reduction will be larger still in a portal environment with a path-loss exponent above two. The same tendency, that cascaded fading shortens the reliable read range relative to a single-path assumption, has been obtained from tag detection probability analysis for both monostatic and bistatic configurations [16]. A link budget built on a one-way channel model therefore risks an antenna layout that is inadequate for a *dyadic* system. The drop in the penalty from 8.2 dB to 5.4 dB on the *Rician* channel has a physical explanation: the line-of-sight component reduces the fading depth on both links at once, so the multiplicative interaction of fading between the links is weakened.

The *dyadic Rician* channel with K = 5 dB requires 22.5 dB, whereas the single *Rayleigh* channel requires 24.1 dB. This does not mean the *dyadic* channel outperforms a single *Rayleigh* channel; the comparison mixes two different variables, the number of links and the type of fading distribution. The benefit of a line-of-sight path on both links outweighs the loss due to the *dyadic* structure. The *dyadic* penalty is therefore meaningful only when compared at the same fading distribution.

### C. *Separability of the Fading Margin and Modulation Choice*

TABLE III. FADING MARGIN RELATIVE TO AWGN AND ITS SENSITIVITY, COMPUTED WITH (7), OVER THE *DYADIC RICIAN* CHANNEL

| K (dB) | ASK margin (dB) | BPSK margin (dB) | BPSK sensitivity, $S_i$ (dB per dB) |
|---|---|---|---|
| 0 | 23.4 | 23.7 | – |
| 4 | 18.0 | 18.0 | 1.43 |
| 6 | 12.9 | 13.1 | 2.45 |
| 8 | 8.2 | 8.1 | 2.50 |
| 10 | 5.0 | 4.9 | 1.60 |
| 12 | 3.0 | 2.9 | 1.00 |
| 15 | 1.5 | 1.5 | 0.47 |
| 20 | 0.5 | 0.4 | 0.22 |

TABLE III lists the ASK and BPSK fading margins, which are almost identical at every value of K, with a maximum deviation of 0.3 dB. A deviation of this size is negligible in practice. It shows that the fading margin depends only on the channel characteristics, while the modulation type sets only the baseline requirement on the AWGN channel. TABLE III also shows the margin shrinking quickly as the K-factor grows, from 23.4 dB at K = 0 dB (linear K = 1, i.e., equal line-of-sight and scattered power, so the margin stays about 2 dB below that of the dyadic Rayleigh channel in TABLE II) to only 0.5 dB at K = 20 dB. This matches the physical picture: the stronger the line-of-sight component, the shallower the fading, and the closer the channel comes to AWGN. Since the fading margin is independent of the modulation, it need be computed only once from the portal geometry and can then be applied to whichever modulation the tag uses. Modulation selection and antenna-geometry design can thus be carried out separately when setting parameters. The consistency of these results also serves as a further check that the simulated system model behaves as theory predicts.

### D. *Effect of the Rician Factor and the Design Threshold*

Fig. 4 shows the BER curves of the *dyadic Rician* channel for eight values of the K-factor. Two trends appear as K increases. The curves shift to the left, indicating that less $E_b/N_0$ is needed to reach the same BER, and their slope steepens toward the AWGN characteristic. Both indicate that a stronger line-of-sight path means less fading on the signal. The sensitivity of the fading margin to the K-factor is given in the last column of TABLE III, expressed as the margin improvement per 1 dB increase in K relative to the K value in the preceding row, computed with (7) from the BPSK margins as described in Section II.D.

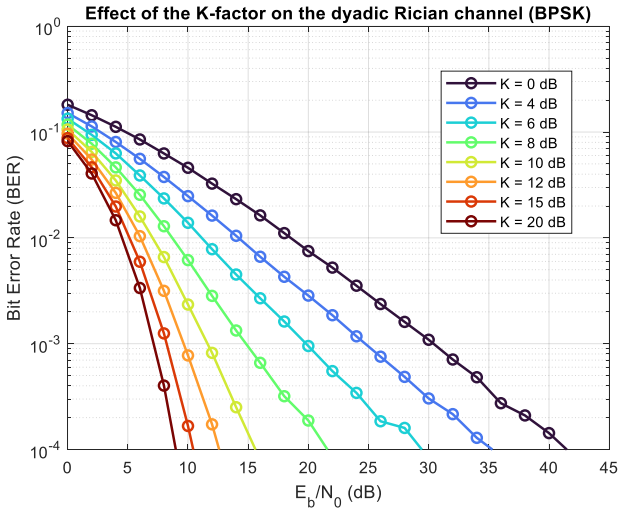



Fig. 4. Effect of the *Rician* factor on the BER of the *dyadic Rician* channel (BPSK)

Sensitivity peaks in the range K = 6 to 8 dB, at 2.50 dB per dB. This marks the inflection point of the margin curve, the range with the fastest rate of improvement. Beyond it, sensitivity falls steadily to just 0.22 dB per dB in the range K = 15 to 20 dB. The curve begins to saturate around K = 12 dB; beyond it, in the range K = 12 to 15 dB, sensitivity drops below 0.5 dB per dB. Keeping the fading margin below 5 dB requires K of at least 10 dB; below 3 dB requires K of at least 12 dB; and below 1.5 dB requires K of at least 15 dB. At K = 20 dB only 0.4 dB of margin remains, meaning the penalty of the *dyadic* structure has practically vanished and the channel behaves almost like AWGN.

These results carry a clear practical implication for toll portal design. The factor K can be raised by physical means,

for instance by aiming the reader antenna beam directly at the tag position on the windshield and clearing obstructions around the portal. Such measures pay off most while K is still below about 12 dB, since in that range every increase in K yields a large margin improvement. Above that value, further spending to strengthen the line-of-sight path is no longer matched by the margin gained. This threshold should be read as a design target for the portal geometry rather than a parameter that stays fixed over time, since channel measurements in vehicular environments show the K-factor varying in time and frequency as the number of active scatterers around the path changes [20].

### *E. Link Correlation and Diversity Order Reduction*

Fig. 5 shows the BER curves of the *dyadic Rayleigh* channel at four values of link envelope correlation. Increasing correlation shifts the curves steadily to the right, and the fully correlated curve ($\rho = 1$) never reaches the target BER within the 50 dB simulation range, flattening out instead. The partially correlated curves ($\rho$ = 0.3 and $\rho$ = 0.6) remain parallel to the uncorrelated curve ($\rho = 0$). TABLE IV summarizes the $E_b/N_0$ required at a BER of $10^{-3}$. The bistatic configuration with zero correlation requires 32.6 dB for BPSK, while correlations of 0.3 and 0.6 raise this to 35.1 dB and 38.1 dB. The ASK–BPSK gap stays between 6.0 and 6.2 dB at every point, so the correlation penalty is independent of the modulation scheme.

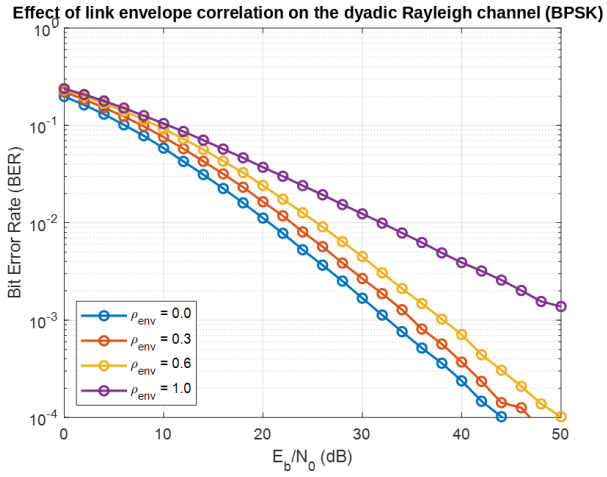



Fig. 5. Effect of link envelope correlation on the *dyadic Rayleigh* channel (BPSK)

TABLE IV. REQUIRED $E_B/N_0$ AT A BER OF 0.001 VERSUS LINK ENVELOPE CORRELATION

| Envelope correlation | ASK (dB) | BPSK (dB) | BPSK penalty (dB) |
|---|---|---|---|
| 0.0 | 38.8 | 32.6 | reference |
| 0.3 | 41.2 | 35.1 | 2.5 |
| 0.6 | 44.1 | 38.1 | 5.5 |
| 1.0 | above 50 | about 52 | about 19 |

The flattening of the fully correlated curve can be understood as follows: in a monostatic reader the forward and return links traverse the same physical path, so the effective channel coefficient becomes the square of the forward-link coefficient, normalized by the square root of two to keep unit mean power. Physically, the signal passes through the same path twice, so every momentary fade is suffered twice over.

In Fig. 5 the curves for ρ = 0, 0.3, and 0.6 run parallel with a slope of about 10 dB per BER decade, i.e., a diversity order of one, so partial correlation merely shifts the curve to the right by 2.5 to 5.5 dB on top of the 8.2 dB *dyadic* penalty and can be made up with more power. The ρ = 1.0 (monostatic) curve, by contrast, is shallow, with a slope of about 18.7 dB per decade, i.e., a diversity order of 0.5; its penalty grows from 19 dB at a BER of $10^{-3}$ to about 29 dB at $10^{-4}$, at which point compensating with power is no longer practical. This is what makes separate transmit and receive antennas at a toll portal a design requirement rather than an optimization choice. The result also puts a number on the monostatic loss that Griffin and Durgin previously described only qualitatively [5]. In the recent literature, the monostatic loss is addressed by adding antennas at the tag and reader together with space-time codes designed specifically for backscatter channels [21], [22]; those options lie outside the single-antenna passive tag considered here.

### *F. Performance Comparison of ASK and BPSK*

A direct comparison of the two modulations can be read from the difference between the ASK and BPSK columns in TABLE II for the five channel models and in TABLE IV for the four correlation values. The difference stays within a narrow band for both the *dyadic Rayleigh* and the single *Rayleigh* channel, confirming that the BPSK advantage is unaffected by the channel structure.

BPSK consistently outperforms ASK by 6.0 dB across every channel model, correlation value, and *Rician* factor tested. This advantage is set by the constellation geometry, not by the channel. The finding agrees with Evecan [19], and adds that the size of the advantage is unchanged when the channel is modeled as *dyadic*. BPSK requires phase control in the tag's impedance-modulation circuit, whereas ASK only needs to switch the impedance magnitude; on a passive tag with a very tight power budget, the extra circuitry can eat into the power saved. A similar consideration arises in work on coded backscatter modulation, which shows that the choice of modulation on a passive tag cannot be separated from the power budget and the complexity of the impedance modulator [23]. Several limitations of the study should also be noted. Using $10^6$ bits per point limits the resolution of the BER estimate to about $10^{-4}$. Detection is assumed coherent with perfect channel knowledge, whereas commercial readers are generally non-coherent, so these results are an optimistic performance bound. The closed-form BER analysis of non-coherent detection over double Rayleigh channels [24] and the detection and performance framework for ambient backscatter systems [25] offer a route to extending the model to non-coherent schemes. Fading is assumed flat and static over one bit interval, so the Doppler effect of a fast-moving vehicle is not accounted for.

## IV. CONCLUSION

Modeling a passive UHF RFID channel as a single path underestimates the required power by 8.2 dB for BPSK and 8.4 dB for ASK without a line-of-sight component, equivalent to a read-range loss of about 38 percent on the two-way path scale, so the *dyadic* model should be used to keep link-budget calculations from promising more range than is actually available. The fading margin relative to the

AWGN channel is independent of the modulation type, with a maximum deviation of 0.3 dB, so the link budget can be decomposed into a modulation term and a channel term that are designed separately. The sensitivity of the fading margin to the *Rician* factor peaks between K = 6 and 8 dB and falls sharply above 12 dB, so toll portals should be designed with antenna placement and geometry that hold K at 12 dB or more to keep the margin below 3 dB. Full inter-link correlation in a monostatic reader reduces the diversity order from 1 to 0.5 with a penalty of about 19 dB at a BER of $10^{-3}$; unlike the constant shift of the *dyadic* structure penalty, this correlation penalty grows as the target BER is tightened, which makes separate transmit and receive antennas a design requirement rather than an optimization choice. Future work should cover non-coherent detection, which better represents commercial readers, different *Rician* factors on the forward and return links, the effect of Doppler shift for fast-moving vehicles, and experimental verification at an operating toll gate.

## ACKNOWLEDGMENT

The authors thank the Telecommunication Engineering Study Program, Telkom University Jakarta, and the Department of Electrical Engineering, State Polytechnic of Malang, for the facilities used to carry out the simulations in this study.

## REFERENCES

[1] A. Budiharjo and S. R. Margarani, "Kajian Penerapan Multi Lane Free Flow (MLFF) di Jalan Tol Indonesia," Jurnal Keselamatan Transportasi Jalan, vol. 6, no. 2, 2019, https://doi.org/10.46447/ktj.v6i2.27.

[2] J. D. Griffin and G. D. Durgin, "Complete Link Budgets for Backscatter-Radio and RFID Systems," IEEE Antennas and Propagation Magazine, vol. 51, no. 2, pp. 11-25, 2009, https://doi.org/10.1109/MAP.2009.5162013.

[3] K. Finkenzeller, RFID Handbook: Fundamentals and Applications in Contactless Smart Cards, Radio Frequency Identification and Near-Field Communication, 3rd ed. Chichester: John Wiley & Sons, 2010, https://doi.org/10.1002/9780470665121.

[4] D. M. Dobkin, The RF in RFID: UHF RFID in Practice, 2nd ed. Oxford: Newnes, 2012. [Online]. Available: https://www.sciencedirect.com/book/9780123945839/the-rf-in-rfid.

[5] J. D. Griffin and G. D. Durgin, "Gains for RF Tags Using Multiple Antennas," IEEE Transactions on Antennas and Propagation, vol. 56, no. 2, pp. 563-570, 2008, https://doi.org/10.1109/TAP.2007.915423.

[6] J. Salo, H. M. El-Sallabi, and P. Vainikainen, "The Distribution of the Product of Independent Rayleigh Random Variables," IEEE Transactions on Antennas and Propagation, vol. 54, no. 2, pp. 639-643, 2006, https://doi.org/10.1109/TAP.2005.863087.

[7] C. Boyer and S. Roy, "Backscatter Communication and RFID: Coding, Energy, and MIMO Analysis," IEEE Transactions on Communications, vol. 62, no. 3, pp. 770-785, Mar. 2014, https://doi.org/10.1109/TCOMM.2013.120713.130417.

[8] N. Van Huynh, D. T. Hoang, X. Lu, D. Niyato, P. Wang, and D. I. Kim, "Ambient Backscatter Communications: A Contemporary Survey," IEEE Communications Surveys & Tutorials, vol. 20, no. 4, pp. 2889-2922, 2018, https://doi.org/10.1109/COMST.2018.2841964.

[9] T. Jiang, Y. Zhang, W. Ma, M. Peng, Y. Peng, M. Feng, and G. Liu, "Backscatter Communication Meets Practical Battery-Free Internet of Things: A Survey and Outlook," IEEE Communications Surveys & Tutorials, vol. 25, no. 3, pp. 2021-2051, 2023, https://doi.org/10.1109/COMST.2023.3278239.

[10] F. Rezaei, C. Tellambura, and S. Herath, "Large-Scale Wireless-Powered Networks with Backscatter Communications—A Comprehensive Survey," IEEE Open Journal of the Communications Society, vol. 1, pp. 1100-1130, 2020, https://doi.org/10.1109/OJCOMS.2020.3012466.

[11] A. Goldsmith, Wireless Communications. Cambridge: Cambridge University Press, 2005, https://doi.org/10.1017/CBO9780511841224.

[12] T. S. Rappaport, Wireless Communications: Principles and Practice, 2nd ed. Upper Saddle River: Prentice Hall, 2002.

[13] F. M. Cahyaningtyas and E. Y. D. Utami, "Simulasi Perbandingan Konfigurasi Patch EMA dengan EMB pada Antena Mikrostrip Elips untuk Pembaca RFID Frekuensi UHF," Jurnal Telematika, vol. 14, no. 2, pp. 51-58, 2019. [Online]. Available: https://journal.ithb.ac.id/telematika/article/view/270.

[14] T. D. Hakim and M. A. Munandar, "Analisa Pengaruh Konfigurasi Power dan Sudut Antena RFID terhadap Jarak Pembacaan dari Automatic Lane Barrier (ALB) ke Tag RFID Kendaraan," Jurnal Elektro, vol. 11, no. 2, pp. 182–189, Jul. 2023. [Online]. Available: https://jurnalteknik.unkris.ac.id/index.php/jie/article/view/274.

[15] V. P. Handayani, K. Quzwain, and A. Novfitri, "Evaluasi Performa Transmisi Sinyal RFID UHF pada Sistem Pembayaran Tol Multi Lane Free Flow," e-Proceeding of Engineering, vol. 12, no. 5, pp. 8050-8052, Oct. 2025. [Online]. Available: https://openlibrarypublications.telkomuniversity.ac.id/index.php/engineering/article/view/27972.

[16] A. Bekkali, S. Zou, A. Kadri, M. Crisp, and R. V. Penty, "Performance Analysis of Passive UHF RFID Systems Under Cascaded Fading Channels and Interference Effects," IEEE Transactions on Wireless Communications, vol. 14, no. 3, pp. 1421-1433, Mar. 2015, https://doi.org/10.1109/TWC.2014.2366142.

[17] J. G. Proakis and M. Salehi, Digital Communications, 5th ed. New York: McGraw-Hill, 2008.

[18] GS1, EPC Radio-Frequency Identity Protocols Generation-2 UHF RFID Standard, Release 2.1, Ratified. Brussels: GS1 AISBL, Jul. 2018. [Online]. Available: https://ref.gs1.org/standards/gen2/2.1.0/.

[19] K. Evecan, "Passive RFID Uplink and Downlink Link Budget and Comparison of ASK and BPSK Backscatter Modulations," Sakarya University Journal of Science, vol. 23, no. 1, pp. 66-75, Feb. 2019, https://doi.org/10.16984/saufenbilder.434517.

[20] L. Bernadó, T. Zemen, F. Tufvesson, A. F. Molisch, and C. F. Mecklenbräuker, "Time- and Frequency-Varying K-Factor of Non-Stationary Vehicular Channels for Safety-Relevant Scenarios," IEEE Transactions on Intelligent Transportation Systems, vol. 16, no. 2, pp. 1007-1017, Apr. 2015, https://doi.org/10.1109/TITS.2014.2349364.

[21] C. He, S. Chen, H. Luan, X. Chen, and Z. J. Wang, "Monostatic MIMO Backscatter Communications," IEEE Journal on Selected Areas in Communications, vol. 38, no. 8, pp. 1896-1909, Aug. 2020, https://doi.org/10.1109/JSAC.2020.3000823.

[22] H. Luan, X. Xie, L. Han, C. He, and Z. J. Wang, "A Better than Alamouti OSTBC for MIMO Backscatter Communications," IEEE Transactions on Wireless Communications, vol. 21, no. 2, pp. 1117-1131, Feb. 2022, https://doi.org/10.1109/TWC.2021.3102111.

[23] C. Boyer and S. Roy, "Coded QAM Backscatter Modulation for RFID," IEEE Transactions on Communications, vol. 60, no. 7, pp. 1925-1934, Jul. 2012, https://doi.org/10.1109/TCOMM.2012.051012.110317.

[24] C. He and Z. J. Wang, "Closed-Form BER Analysis of Non-Coherent FSK in MISO Double Rayleigh Fading/RFID Channel," IEEE Communications Letters, vol. 15, no. 8, pp. 848-850, Aug. 2011, https://doi.org/10.1109/LCOMM.2011.061011.110276.

[25] G. Wang, F. Gao, R. Fan, and C. Tellambura, "Ambient Backscatter Communication Systems: Detection and Performance Analysis," IEEE Transactions on Communications, vol. 64, no. 11, pp. 4836-4846, Nov. 2016, https://doi.org/10.1109/TCOMM.2016.2602341.